Homo-Oligomerization Facilitates the Interferon-Antagonist Activity of the Ebolavirus VP35 Protein

St. Patrick Reid, **Washington B. Cárdenas**, and **Christopher F. Basler**[1]
Department of Microbiology, Mount Sinai School of Medicine, New York, New York 10029

Abstract

We have identified a putative coiled-coil motif within the amino-terminal half of the ebolavirus VP35 protein. Cross-linking studies demonstrated the ability of VP35 to form trimers, consistent with the presence of a functional coiled-coil motif. VP35 mutants lacking the coiled-coil motif or possessing a mutation designed to disrupt coiled-coil function were defective in oligomerization, as deduced by co-immunoprecipitation studies. VP35 inhibits signaling that activates interferon regulatory factor 3 (IRF-3) and inhibits (IFN)-α/β production. Experiments comparing the ability of VP35 mutants to block IFN responses demonstrated that the VP35 amino-terminus, which retains the putative coiled-coil motif, was unable to inhibit IFN responses, whereas the VP35 carboxy-terminus weakly inhibited the activation of IFN responses. IFN-antagonist function was restored when a heterologous trimerization motif was fused to the carboxy-terminal half of VP35, suggesting that an oligomerization function at the amino-terminus facilitates an "IFNantagonist" function exerted by the carboxy-terminal half of VP35.

Ebola virus infection can cause severe hemorrhagic fever in human and non-human primates (Sanchez et al., 2001). The molecular mechanisms of ebolavirus pathogenesis remain incompletely understood although several potential mechanisms contributing to virulence have been reviewed (Mahanty and Bray, 2004). These mechanisms include cytotoxicity of the viral glycoprotein (GP), the production of pro-inflammatory cytokines and the disregulation of the coagulation cascade due to the production of tissue factor (Chan, Ma, and Goldsmith, 2000; Geisbert et al., 2003a; Geisbert et al., 2003b; Sullivan et al., 2005; Volchkov et al., 2001; Yang et al., 2000). Each of these processes, however, likely occurs as a result of the active replication of the virus. Thus, the ability of the virus to counteract early antiviral responses, including the interferon (IFN)-α/β system, is likely to play an important role in ebolavirus virulence (Mahanty and Bray, 2004).

Several studies have demonstrated that ebolavirus infection inhibits host IFN responses, preventing infected cells from responding to IFN and also impairing IFN production (Gupta et al., 2001; Harcourt, Sanchez, and Offermann, 1998; Harcourt, Sanchez, and Offermann, 1999). Expression of the VP35 protein of either Zaire ebolavirus or Reston ebolavirus inhibited host cell interferon-α/β (IFN α/β) responses (Basler et al., 2000; Basler et al. 2003). VP35 can functionally substitute for another viral "IFN-antagonist," the influenza A virus NS1 protein and can inhibit production of IFN β induced by several stimuli, including Sendai virus (SeV) infection or dsRNA transfection (Basler et al., 2000). Inhibition of host IFN responses appears to occur, at least in part, because VP35 is able to prevent the phosphorylation that leads to the activation of interferon regulatory factor 3 (IRF-3) (Basler et al., 2003), a cellular transcription factor that plays a critical role in the virus-mediated activation of the IFN α/β gene (Schafer et al., 1998; Wathelet et al., 1998; Weaver, Kumar,

[1]Corresponding Author: Christopher F. Basler, PhD, Assistant Professor, Dept. Microbiology, Box 1124, Mount Sinai School of Medicine, 1 Gustave L. Levy Place, New York, NY 10029, Tel (212) 241-4847, Fax (212) 534-1684, chris.basler@mssm.edu.

and Reich, 1998). Consistent with these observations, ebolavirus infection does not activate IRF-3 (Basler et al., 2003). VP35, expressed from an alphavirus vector, also inhibited production of IFN in human dendritic cells (Bosio et al., 2003), and mutation of specific basic residues within the carboxy-terminal half of VP35 impairs its ability to inhibit Sendai virus-induced IFN α/β responses (Hartman, Towner, and Nichol, 2004).

In addition to its IFN-antagonist activity, VP35 is an essential component of the viral RNA-dependent RNA polymerase complex, where it is an ortholog of paramyxovirus and rhabdovirus phosphoproteins. VP35 also plays an important structural role in the virus (Huang et al., 2002; Muhlberger et al., 1998; Watanabe et al., 2004). Despite its importance for ebolavirus replication, relatively little information is available regarding functionally important regions of VP35.

The present study demonstrates that VP35 forms homooligomers and that a putative coiled-coil domain within the amino-terminal half of VP35 is required for this property. Further, we demonstrate that although the carboxy-terminal half of VP35 contains sequences sufficient to inhibit Sendai virus-induced IFN α/β responses, oligomerization is required for full VP35 "IFN-antagonist function."

Results

The Zaire ebolavirus VP35 protein forms oligomers

The amino acid sequence of Zaire ebolavirus VP35 was analyzed with COILS, a computer program that predicts coiled-coil domains (Lupas, Van Dyke, and Stock, 1991). COILS predicted with high probability a single coiled-coil domain between amino acids 82–118 of the 340 amino acid of the VP35 protein (Fig. 1A). Thus, we hypothesized that the predicted coiled-coil domain may mediate VP35 oligomerization.

To address the possibility that VP35 oligomerizes, FLAG-tagged VP35 (FLAG-VP35) was partially purified from transfected cells and fractionated on a Superdex-200 gel filtration column. Column fractions were collected and analyzed by SDS-PAGE. Silver staining and western blot analysis revealed that VP35 eluted in four fractions with a peak in the 126–194 kDa range, suggesting the formation of a trimeric-tetrameric complex (Fig. 1B). Silver stained gels did not show detectable co-purifying proteins, suggesting that VP35 forms homo-oligomers (Fig. 1B).

The oligomeric form of the purified Flag-VP35 was further analyzed following crosslinking with Dithiobis(succinimidylpropionate) (DSP). The partially purified Flag-VP35 was mock-treated or treated with 1, 2 or 5 μM DSP following standard procedures, then briefly centrifuged and analyzed by western blot with an anti-VP35 antibody (Fig. 1C). After cross-linking with either 1 or 2 μM DSP, VP35 migrated at an apparent molecular weight of approximately 124 kDa (based on the migration of the band in the 2 μM lane). This observation is most consistent with the formation of VP35 homo-trimers (Fig. 1C). Notably, however, increasing the DSP concentration reproducibly resulted in a loss in the amount of VP35 protein visible on gels (Fig. 1C). This suggests that, in addition to trimers, larger aggregates of VP35 were also cross-linked such that they were too large to enter the gel. Given that significant amounts of VP35 in a form larger than 200 kDa were not detected during gel filtration experiments (Fig. 1B), it is likely that the majority of VP35 is trimeric. However, it should also be noted that under the non-reducing electrophoresis conditions used to analyze the mock cross-linked VP35, variable amounts of higher molecular weight forms were detected, although what these form represent in terms of the oligomeric state of VP35 is unclear (Fig. 1C). Based on these results, we conclude that VP35 forms trimers, but we cannot exclude the formation of additional higher-order oligomers as well.

The predicted coiled-coil domain is required for oligomer formation

To determine whether the predicted coiled-coil domain is required for VP35 oligomer formation, several VP35 mutants were constructed (Fig. 2A) and screened for their ability to interact with wild-type VP35 (Fig. 2B). Coimmunoprecipitation analysis demonstrated that FLAG-VP35 interacted with both full-length HA-VP35 and with HA-VP35$_{1-170}$, a truncation mutant containing the predicted coiled-coil domain but lacking amino acids 171–340 (Fig. 2B, lanes 2 and 5). In contrast, HAVP35$_{171-340}$, lacking the amino-terminal 170 amino acids, did not detectably interact with FLAGVP35 (Fig2B, lane 6). Mutant, HA-VP35Δ_{82-118}, deleted of the predicted coiled-coil domain, was also unable to interact with FLAG-VP35 (Fig. 2B, lane 3). An additional mutant, HAVP35$_{L90/93/107A}$, in which key leucines in the "a" and "d" positions of the predicted coiled-coil domain were substituted with alanine, was also unable to interact with FLAG-VP35 (Fig. 2B, lane 4). Expression of each of the proteins analyzed in this experiment was confirmed by western blot (Fig. 2B). Notably, when total lysates were probed with anti-HA antibody, multimeric forms of VP35 molecules were seen in those lanes containing either full-length VP35 or the amino-terminal half of VP35. In contrast, VP35 mutants lacking the coiled-coil domain or possessing a mutant coiled-coil domain do not produce slower migrating forms, suggesting that they have lost their ability to form SDS-stable oligomers.

Using constructs analogous to those used for the co-immunoprecipitation experiments, coiled-coil domain mediated interactions were further validated using the mammalian two-hybrid system (data not shown). Thus, the predicted coiled-coil domain contributes to VP35 oligomer formation.

Oligomer formation is required for full IFN antagonist function

We have previously demonstrated that VP35 can inhibit the SeV-induced activation the IRF-3 responsive promoter ISG54 (Basler et al., 2000). We therefore assessed the IFN-antagonist function of VP35 mutants with this assay. 293T cells were transfected with an ISG54-CAT reporter, a constitutively expressed *Renilla* luciferase plasmid pRL-tk (Promega) and expression plasmids. The expression plasmids included an empty vector, a plasmid encoding wild type VP35 and plasmids encoding the two truncation mutants, HA-VP35$_{1-170}$ and HA-VP35$_{171-340}$. Twenty-four hours post-transfection, the cells were either mock infected or infected with Sendai virus (SeV), a potent activator of IRF-3, at multiplicity of infection of 10. Subsequently, ISG54-CAT reporter activity was determined and normalized to *Renilla* luciferase activity. Infection of cells transfected with empty vector resulted in a striking up-regulation of this IRF-3 responsive reporter (Fig. 3A). As previously reported, wild type VP35 was able to inhibit reporter activation. Interestingly, when transfected in relatively large amounts (2.5 μg/10^6 cells) the oligomerization-deficient mutant HA-VP35$_{171-340}$ inhibited activation of the reporter, while HAVP35$_{1-170}$, which retained an ability to interact with full-length VP35 (Fig. 2B), was unable to inhibit activation of the reporter (Fig. 3A).

Although HA-VP35$_{171-340}$ retained some function as an IFN antagonist when large amounts of plasmid were transfected, it was of interest to determine whether VP35 oligomer formation, mediated by the amino-terminus of VP35, contributes to its IFN antagonist function. Thus, a heterologous trimerization domain, the "foldon" domain, was fused to HA-VP35$_{171-340}$ (Fig. 2A). The foldon trimerization domain is a small globular domain derived from the carboxy-terminus of bacteriophage T4 fibritin protein which has been demonstrated to mediate trimerization when fused to heterologous proteins (e.g (Frank et al., 2001; Stevens et al., 2004). The foldon domain was fused to the amino terminus of HA-VP35$_{171-340}$ (Foldon-HA-VP35$_{171-340)}$, and the ability of the this construct to inhibit virus-induced activation of the reporter was compared to the IFN-antagonist activities of full-

length VP35 and to VP35$_{171-340}$. Addition of the foldon domain enhanced the IFN-antagonist activity of the VP35 carboxy-terminus (Fig. 3B). This difference is most easily seen when the amounts of protein produced by the various constructs are compared. The Foldon-VP35 plasmid produces modestly more protein/microgram of plasmid DNA than either wild-type VP35 or HA-VP35$_{171-340}$. However, the Foldon-HA-VP35$_{171-340}$ 25 ng sample (where relatively little protein is present) displays an IFN-antagonist activity at least as strong as that seen in the 250 ng HA-VP35$_{171-340}$ sample (where much more protein is present). Thus, these data support the conclusion that the foldon domain restores activity to the carboxy-terminal half of VP35 (Fig. 3C). As a control, the foldon domain was fused to the amino-terminus of VP35$_{1-170}$. When this construct was tested for IFN-antagonist activity with the same reporter gene assay, it exhibited no ability to inhibit SeV-induced gene expression (data not shown). Thus, the foldon domain does not appear to act, on its own, as an IFN-antagonist. That the foldon domain restores the ability of the carboxyterminal half of VP35 to oligomerize is supported by SDS-PAGE analysis of samples that were not boiled prior to electrophoresis, where the foldon domain construct yields higher molecular weight bands (Fig. 3D).

To determine whether these constructs also inhibit production of endogenous IFN, an IFN bioassay was performed. 293T cells were transfected with different amounts of either empty vector or plasmids expressing wild type VP35, VP35$_{171-340}$ or Foldon-VP35$_{171-340}$. One day post-transfection, the cells were infected with SeV (moi=10). One day following this infection, supernatants were harvested, clarified by centrifugation and exposed to ultraviolet (UV) light to inactivate infectious virus. A series of two-fold dilutions of these UV inactivated supernatants were then added to Vero cells. One day post-treatment, the Vero cells were infected with a green fluorescence protein (GFP) –expressing Newcastle disease virus (NDVGFP). The presence of IFN in the supernatants of the transfected 293T cells, leads to suppression of NDV-GFP replication and hence to loss of GFP expression. This is illustrated in Fig. 4A where the supernatants from empty vector–transfected, SeV-infected 293T cells induce in Vero cells an antiviral state (see empty vector (2500 ng) panels, top). When neutralizing anti-IFNβ antibody was added to the supernatants from the empty vector-treated, SeV-infected 293T cells, the antiviral effect was lost, demonstrating that, in this experiment, the antiviral effect is mediated by IFN β (Fig. 4, anti-IFN β panel).

When the different VP35 constructs were assessed, significant suppression of IFN production was evident even in the supernatants of cells transfected with as little as 25 ng of VP35- or Foldon-VP35$_{(171-340)}$ expression plasmid (see VP35 and Foldon-VP35$_{(171-340)}$ columns) (Fig. 4A). In contrast, VP35$_{(171-340)}$ only detectably suppressed IFN production when 2500 ng of plasmid were transfected (Fig. 4A). Thus, in this assay, the Foldon-VP35$_{(171-340)}$ construct is 100-times more potent than the VP35$_{(171-340)}$ plasmid.

The relative ability of these mutants to affect activation of an endogenous, IRF-3 responsive gene, the ISG56 gene (Grandvaux et al., 2002), was also addressed (Fig. 4B). Western blotting for the protein P56, the product of the ISG56 gene (Guo, Peters, and Sen, 2000), was performed using an anti-p56 polyclonal antiserum. Virus-induced p56 expression was inhibited in cells transfected with as little as 25 ng of either full-length VP35 plasmid or Foldon-HA-VP35$_{171-340}$ plasmid. In contrast, 2.5 μg of HA-VP35$_{171-340}$ plasmid was required to achieve comparable levels of inhibition (Fig. 4B). It should be noted that none of the constructs brought p56 expression levels to the baseline seen in empty vector-transfected, mock infected cells. This reflects the fact that transfection efficiencies are not 100 percent resulting in the presence of a pool of cells that do not receive any VP35 plasmid. In summary, these data are consistent with the ability of the Foldon domain to restore activity to the carboxy-terminal half of VP35.

To address the mechanism by which the foldon domain restores the IFN-antagonist activity of VP35$_{171-340}$, the activation status of IRF-3 was examined. Upon viral stimulation, the transcription factor IRF-3 is phosphorylated by virus-activated kinases (Fitzgerald et al., 2003; Sharma et al., 2003). Phosphorylated IRF-3 then homodimerizes and is translocated to the nucleus where cofactors such as CBP/p300 are recruited to initiate transcription of target genes (Servant, Grandvaux, and Hiscott, 2002). Previously we have shown that VP35 can prevent IRF-3 phosphorylation, IRF-3 dimerization and thus IRF-3 activation (Basler et al., 2003). Similarly, Foldon-HA-VP35$_{171-340}$ displays the ability to inhibit IRF-3 dimer formation at levels comparable to full-length HA-VP35 (Fig. 5). Although HA-VP35$_{171-340}$ was also able to inhibit dimer formation in comparison to the empty vector-infected cells, the inhibition was significantly less than that seen with either full-length VP35 or with Foldon-HA-VP35$_{171-340}$. Thus the ability of these constructs to inhibit IRF-3 correlates with their ability to inhibit IFN β promoter activation, IFN β production and p56 expression. Although we correlate this activity with inhibition of IRF-3, we cannot exclude the possibility that VP35 also targets other components of the IFN response as well. Taken together, these data indicate that the carboxy-terminus of VP35 exhibits partial IFN antagonist function and that oligomerization enhances this activity.

Discussion

Numerous antagonists of the IFN response have now been described, including many encoded by negative-strand RNA viruses (Garcia-Sastre, 2004). The biological significance of such molecules is highlighted by their importance for virulence and virus host range. For example, mutants of influenza A viruses (Garcia-Sastre et al., 1998), bunyamwera virus (Bridgen et al., 2001), vaccinia virus (Brandt and Jacobs, 2001), herpes simplex virus type 1 (HSV-1) (Chou et al., 1990; Leib et al., 1999) and Rift Valley Fever virus (Bouloy et al., 2001) which lack or which possess altered viral interferon-antagonists, are attenuated in mice. In addition, species-specific abilities to counteract host interferon responses have been demonstrated for several paramyxoviruses (e.g. (Bossert and Conzelmann, 2002; Parisien, Lau, and Horvath, 2002; Park et al., 2003; Young et al., 2001). Because of their importance for virulence, IFN-antagonists could potentially serve as targets for novel antivirals, and mutagenesis of IFN-antagonists has been suggested as a strategy for the rational generation of live, attenuated vaccine strains (Garcia-Sastre, 2004).

The present study demonstrates that VP35 multimerizes, forming homotrimers, that a putative coiled-coil domain appears to be required for efficient homooligomerization and that this region facilitates the "IFN-antagonist" function of the protein. The carboxy-terminal half of VP35 contained sequences that were sufficient, when fused even to a heterologous trimerization motif, to fully inhibit IRF-3 activation. Our data are consistent with the observations of Hartman et al. who found that mutation of individual basic residues within the VP35 carboxy-terminus impaired VP35 function (Hartman, Towner, and Nichol, 2004). However, this previous study did not exclude a requirement for amino-terminal portions of VP35 in this function. Our data clearly demonstrate that the carboxy-terminal half of VP35 has sufficient information to prevent activation of IRF-3, provided an oligomerization function is present. The method described here, fusion of a heterologous oligomerization motif to deletion mutants of VP35, should facilitate the further definition of a minimal "IFN-antagonist domain."

These observations regarding the regions of VP35 required for its IFN-antagonist activity have implications for the mechanism by which VP35 blocks IFN responses and for the generation of ebolaviruses lacking this function. Although the precise targets of VP35 remain to be defined, our previous data indicates that VP35 can inhibit virus-induced IRF-3 activation. With our present observations, we can hypothesize that the carboxy-terminal half

of VP35 interacts with a component(s) of the virus–induced pathways activating IRF-3 and that oligomerization stabilizes this interaction. Recently identified proteins that can be considered candidate targets of VP35 include the cellular RNA helicases RIG-I and MDA-5. These proteins appear to participate in the detection of virus infection and in the subsequent activation of IRF-3 (Andrejeva et al., 2004; Sumpter et al., 2005; Yoneyama et al., 2004). Interestingly, the V proteins of several paramyxoviruses were found to inhibit signaling by MDA-5 and to interact with MDA-5 (Andrejeva et al., 2004), explaining their ability to inhibit IFN β production (He et al., 2002; Poole et al., 2002). In addition, RIG-I regulates permissiveness of cells for hepatitis C virus (HCV) replicons, and the HCV NS3/4A protease inhibits RIG-I signaling (Foy et al., 2005). It will of interest to determine whether VP35 interacts with these cellular proteins and whether multimerization of VP35 is required for any such interactions.

As noted above, VP35 is multifunctional. In addition to its anti-IFN properties, it is analogous to the phosphoprotein (P) of rhabdoviruses and paramyxoviruses in that it is encoded at the same position within genome (i.e by the gene which follows the nucleoprotein (N) gene) and because it acts as a co-factor for the viral RNA-dependent RNA polymerase in the transcription and replication of viral genes (Muhlberger et al., 1998). Like VP35, paramyxovirus and rhabdovirus P proteins possess coiled-coil domains. The coiled-coil domains of the paramyxovirus P proteins reportedly mediate formation of homotrimers or homotetramers, which parallels our observations with VP35 (Choudhary et al., 2002; Curran et al., 1995; Rahaman et al., 2004; Tarbouriech et al., 2000). The ability of P proteins to oligomerize appears to be of functional importance for paramyxovirus RNA synthesis (e.g) (Choudhary et al., 2002; Rahaman et al., 2004). It will also be of interest to determine whether the coiled-coil domain of VP35 is required for ebolavirus RNA synthesis.

The most straightforward means of evaluating the importance of VP35's IFN-antagonist activity will be the generation of recombinant ebolaviruses lacking this activity, and methods exist to generate such recombinant viruses from cDNA (Neumann et al., 2002; Towner et al., 2005; Volchkov et al., 2001). However, the multifunctional nature of VP35 complicates the generation of such a virus. The data described above should facilitate the further definition of those portions of the protein required for this function. The present studies may therefore facilitate the generation of "IFN-antagonist deficient" ebolaviruses.

Materials and Methods

Cells, viruses and plasmids

293T cells were maintained in Dulbecco's modified Eagle medium (DMEM) supplemented with 10% fetal bovine serum (FBS), 100 units/ml penicillin G and 100 μg/ml streptomycin. Sendai virus strain Cantell was grown in 10-day old embryonated chicken eggs at 37°C for 48 hours. The plasmid pCAGGS-HA-VP35 was derived from pcDNA3-EboVP35 (Basler et al., 2000) and was used to generate all HA-VP35 mutants utilized in this study. Additionally, pCAGGS-human IRF-3 was previously described (Basler et al., 2003). A plasmid containing the "Foldon" domain was kindly provided by James Stevens and Ian Wilson (The Scripps Research Institute).

Western Blot analysis

293T cells were transfected using Lipofectamine 2000 (LF2000) (Invitrogen) as previously described (Basler et al., 2003). Briefly, cells were transfected in suspension with 1 μg of pCAGGS-hIRF-3 and 2.5 μg of the indicated expression plasmids. Twenty-four hours post-transfection cells were infected with SeV or mock infected. Ten hours post-infection cell lysates were prepared in a modified RIPA lysis buffer (50 mM Tris-HCl [pH 7.4], 150 mM

NaCl, 1 mM EDTA, 1% NP-40, 0.25% DOC, 1 mM sodium orthovanadate and Roche protease inhibtor cocktail). The lysates were then subjected to native gel electrophoresis as described previously (Iwamura et al., 2001). After electrophoresis IRF-3 was detected by western blot analysis with polyclonal anti-IRF-3 antibody FL-425 (Santa Cruz Biotechnology) diluted 1:500.

Western blot detection of p56 expression was performed with an anti-p56 antibody kindly provided by Dr. Ganes Sen (The Cleveland Clinic Foundation).

Gel Filtration

293T cells were transfected with LF2000 and 3 μg of FLAG-VP35 expression plasmid. Forty-eight hours post-transfection cell lysates were prepared in 0.25 mM Tris-Cl (pH 8.0), 500 mM KCl, 0.5 mM EDTA, 10% glycerol, 1mM DTT, 0.05% Triton X-100 and Roche protease inhibitor cocktail and incubated with 75 μl of a 50% slurry of anti-FLAG-M2 affinity gel (Sigma) for 2 hr at 4°C. FLAG-VP35 was then eluted with 100 μg/ml FLAG peptide (Sigma) in 50 Mm Tris-Cl (pH 8.0), 150 mM NaCl, 10% glycerol, 5 mM DTT and 0.1% SDS. The eluant was loaded onto a Superdex-200 column (Amersham Biosciences). Collected fractions were then subjected to with monoclonal anti-VP35 antibody (6C5) diluted 1:10,000 and to SDS-PAGE and silver stain analysis (Invitrogen).

Cross-linking

293T cells were transfected with LF2000 and 8 μg of FLAG-VP35 expression plasmid. Forty-eight hours post-transfection cell lysates were prepared in 50 mMTris-Cl (pH 8.0), 280 mM NaCl, 0.2 mM EDTA, 2.0 mM EGTA, 10% glycerol, 0.05% Igepal CA-630, 0.1 mM Sodium Orthovanadate, 1 mM DTT and Roche protease inhibitor cocktail and incubated with 75 μl of a 50% slurry of anti-FLAG-M2 affinity gel (Sigma) for 2 hr at 4°C. FLAG-VP35 was then eluted with 100 μg/ml FLAG peptide (Sigma) in the same buffer. The membrane permeable and thiolcleavable crosslinker Dithiobis[succinimydylpropionate] (DSP) (Pierce) was prepared as a 25 mM stock solution in dimethyl sulfoxide (DMSO). The eluant was then incubated for 30 minutes at room temperature with DSP at a final concentration of 0, 1, 2 of 5 mM. The reaction was quenched by the addition of 20 mM Tris-Cl pH 7.5 for 15 min at room temperature. The samples were then subjected to SDS-PAGE analysis under nonreducing conditions and subsequent western blot analysis with monoclonal anti-VP35 antibody (6C5) diluted 1:5000. Molecular weight determinations were made using the AlphaImager 3400, AlphaEase FC software (Alpha Innotech).

Co-immunoprecipitation assays

293T cells were transfected using LF2000 with 2 μg of the indicated expression plasmids. Twenty-four hours post-transfection cell lysates were prepared in modified RIPA lysis buffer (see above) and subsequently incubated with 50 μl of a 50% slurry of anti-FLAG-M2 affinity gel (Sigma) for 2 hr at 4°C. Bound lysates were subjected to western blot analysis with monoclonal anti-HA antibody (Sigma) diluted 1:5000 and M2 anti-FLAG antibody (Sigma) diluted 1:5000.

Reporter gene assays

293T cells were transfected using LF2000 with either 2.5, 0.25 or 0.025 μg of the indicated expression plasmids along with 0.3 μg of the CAT reporter vector pHISG-54-CAT and 0.3 μg of an expression plasmid that constitutively expresses the *Renilla* luciferase reporter vector pRL-tk (Promega). Twenty four hours post-transfection cells were infected with SeV or mock-infected. Twelve hours post-infection cells were analyzed as previously described (Basler et al., 2003).

In addition, cell lysates were subjected to SDS-PAGE and subsequent western blot analysis with polyclonal anti-P56 antiserum diluted 1:2000 or, to verify expression of wildtype VP35, HA-VP35$_{171–340}$ and Foldon-HA-VP35$_{171–340}$, with a monoclonal anti-HA antibody (Sigma).

IFN BIOASSAY

293T cells were transfected with different concentrations of either empty vector or plasmids expressing wild type VP35, VP35$_{(171–340)}$ or Foldon-VP35$_{(171–340)}$. One day post-transfection, the cells were infected with SeV (moi=10). One day following this infection, supernatants were harvested, clarified by centrifugation and exposed to ultraviolet (UV) light to inactivate infectious virus. A series of two-fold dilutions of these UV inactivated supernatants were then added to Vero cells. One day post-treatment, the Vero cells were infected with a green fluorescence protein (GFP) –expressing Newcastle disease virus (NDV-GFP) at an moi=6. The presence of IFN in the supernatants of the transfected and SeV infected 293T cells, leads to suppression of NDV-GFP replication and hence to loss of GFP expression in the treated Vero cells. In contrast, when the IFN response is suppressed by expression of a particular protein or is neutralized by addition of an anti-IFNβ antibody, NDV-GFP replication is restored.

Acknowledgments

References

Andrejeva J, Childs KS, Young DF, Carlos TS, Stock N, Goodbourn S, Randall RE. The V proteins of paramyxoviruses bind the IFN-inducible RNA helicase, mda-5, and inhibit its activation of the IFN-beta promoter. Proc Natl Acad Sci U S A. 2004; 101(49):17264–17269. [PubMed: 15563593]

Basler CF, Mikulasova A, Martinez-Sobrido L, Paragas J, Muhlberger E, Bray M, Klenk HD, Palese P, Garcia-Sastre A. The Ebola virus VP35 protein inhibits activation of interferon regulatory factor 3. J Virol. 2003; 77(14):7945–7956. [PubMed: 12829834]

Basler CF, Wang X, Muhlberger E, Volchkov V, Paragas J, Klenk HD, Garcia-Sastre A, Palese P. The Ebola virus VP35 protein functions as a type I IFN antagonist. Proc Natl Acad Sci U S A. 2000; 97(22):12289–12294. [PubMed: 11027311]

Bosio CM, Aman MJ, Grogan C, Hogan R, Ruthel G, Negley D, Mohamadzadeh M, Bavari S, Schmaljohn A. Ebola and Marburg viruses replicate in monocytederived dendritic cells without inducing the production of cytokines and full maturation. J Infect Dis. 2003; 188(11):1630–1638. [PubMed: 14639532]

Bossert B, Conzelmann KK. Respiratory syncytial virus (RSV) nonstructural (NS) proteins as host range determinants: a chimeric bovine RSV with NS genes from human RSV is attenuated in interferon-competent bovine cells. J Virol. 2002; 76(9):4287–4293. [PubMed: 11932394]

Bouloy M, Janzen C, Vialat P, Khun H, Pavlovic J, Huerre M, Haller O. Genetic evidence for an interferon-antagonistic function of rift valley fever virus nonstructural protein NSs. J Virol. 2001; 75(3):1371–1377. [PubMed: 11152510]

Brandt TA, Jacobs BL. Both carboxy- and amino-terminal domains of the vaccinia virus interferon resistance gene, E3L, are required for pathogenesis in a mouse model. J Virol. 2001; 75(2):850–856. [PubMed: 11134298]

Bridgen A, Weber F, Fazakerley JK, Elliott RM. Bunyamwera bunyavirus nonstructural protein NSs is a nonessential gene product that contributes to viral pathogenesis. Proc Natl Acad Sci U S A. 2001; 98(2):664–669. [PubMed: 11209062]

Chan SY, Ma MC, Goldsmith MA. Differential induction of cellular detachment by envelope glycoproteins of Marburg and Ebola (Zaire) viruses. J Gen Virol. 2000; 81(Pt 9):2155–2159. [PubMed: 10950971]

Chou J, Kern ER, Whitley RJ, Roizman B. Mapping of herpes simplex virus-1 neurovirulence to gamma 134.5, a gene nonessential for growth in culture. Science. 1990; 250(4985):1262–1266. [PubMed: 2173860]

Choudhary SK, Malur AG, Huo Y, De BP, Banerjee AK. Characterization of the oligomerization domain of the phosphoprotein of human parainfluenza virus type 3. Virology. 2002; 302(2):373–382. [PubMed: 12441081]

Curran J, Boeck R, Lin-Marq N, Lupas A, Kolakofsky D. Paramyxovirus phosphoproteins form homotrimers as determined by an epitope dilution assay, via predicted coiled coils. Virology. 1995; 214(1):139–149. [PubMed: 8525609]

Fitzgerald KA, McWhirter SM, Faia KL, Rowe DC, Latz E, Golenbock DT, Coyle AJ, Liao SM, Maniatis T. IKKepsilon and TBK1 are essential components of the IRF3 signaling pathway. Nat Immunol. 2003; 4(5):491–496. [PubMed: 12692549]

Foy E, Li K, Sumpter R Jr, Loo YM, Johnson CL, Wang C, Fish PM, Yoneyama M, Fujita T, Lemon SM, Gale M Jr. Control of antiviral defenses through hepatitis C virus disruption of retinoic acid-inducible gene-I signaling. Proc Natl Acad Sci U S A. 2005; 102(8):2986–2991. [PubMed: 15710892]

Frank S, Kammerer RA, Mechling D, Schulthess T, Landwehr R, Bann J, Guo Y, Lustig A, Bachinger HP, Engel J. Stabilization of short collagen-like triple helices by protein engineering. J Mol Biol. 2001; 308(5):1081–1089. [PubMed: 11352592]

Garcia-Sastre A. Identification and characterization of viral antagonists of type I interferon in negative-strand RNA viruses. Curr Top Microbiol Immunol. 2004; 283:249–280. [PubMed: 15298172]

Garcia-Sastre A, Egorov A, Matassov D, Brandt S, Levy DE, Durbin JE, Palese P, Muster T. Influenza A virus lacking the NS1 gene replicates in interferon-deficient systems. Virology. 1998; 252(2):324–330. [PubMed: 9878611]

Geisbert TW, Hensley LE, Jahrling PB, Larsen T, Geisbert JB, Paragas J, Young HA, Fredeking TM, Rote WE, Vlasuk GP. Treatment of Ebola virus infection with a recombinant inhibitor of factor VIIa/tissue factor: a study in rhesus monkeys. Lancet. 2003a; 362(9400):1953–1958. [PubMed: 14683653]

Geisbert TW, Young HA, Jahrling PB, Davis KJ, Kagan E, Hensley LE. Mechanisms underlying coagulation abnormalities in ebola hemorrhagic fever: overexpression of tissue factor in primate monocytes/macrophages is a key event. J Infect Dis. 2003b; 188(11):1618–1629. [PubMed: 14639531]

Grandvaux N, Servant MJ, tenOever B, Sen GC, Balachandran S, Barber GN, Lin R, Hiscott J. Transcriptional profiling of interferon regulatory factor 3 target genes: direct involvement in the regulation of interferon-stimulated genes. J Virol. 2002; 76(11):5532–5539. [PubMed: 11991981]

Guo J, Peters KL, Sen GC. Induction of the human protein P56 by interferon, double-stranded RNA, or virus infection. Virology. 2000; 267(2):209–219. [PubMed: 10662616]

Gupta M, Mahanty S, Ahmed R, Rollin PE. Monocyte-derived human macrophages and peripheral blood mononuclear cells infected with ebola virus secrete MIP-1alpha and TNF-alpha and inhibit poly-IC-induced IFN-alpha in vitro. Virology. 2001; 284(1):20–25. [PubMed: 11352664]

Harcourt BH, Sanchez A, Offermann MK. Ebola virus inhibits induction of genes by double-stranded RNA in endothelial cells. Virology. 1998; 252(1):179–188. [PubMed: 9875327]

Harcourt BH, Sanchez A, Offermann MK. Ebola virus selectively inhibits responses to interferons, but not to interleukin-1beta, in endothelial cells. J Virol. 1999; 73(4):3491–3496. [PubMed: 10074208]

Hartman AL, Towner JS, Nichol ST. A C-terminal basic amino acid motif of Zaire ebolavirus VP35 is essential for type I interferon antagonism and displays high identity with the RNA-binding domain

of another interferon antagonist, the NS1 protein of influenza A virus. Virology. 2004; 328(2):
177–184. [PubMed: 15464838]

He B, Paterson RG, Stock N, Durbin JE, Durbin RK, Goodbourn S, Randall RE, Lamb RA. Recovery
of paramyxovirus simian virus 5 with a V protein lacking the conserved cysteine-rich domain: the
multifunctional V protein blocks both interferon-beta induction and interferon signaling. Virology.
2002; 303(1):15–32. [PubMed: 12482655]

Huang Y, Xu L, Sun Y, Nabel GJ. The assembly of Ebola virus nucleocapsid requires virion-
associated proteins 35 and 24 and posttranslational modification of nucleoprotein. Mol Cell. 2002;
10(2):307–316. [PubMed: 12191476]

Iwamura T, Yoneyama M, Yamaguchi K, Suhara W, Mori W, Shiota K, Okabe Y, Namiki H, Fujita T.
Induction of IRF-3/-7 kinase and NF-kappaB in response to double-stranded RNA and virus
infection: common and unique pathways. Genes Cells. 2001; 6(4):375–388. [PubMed: 11318879]

Leib DA, Harrison TE, Laslo KM, Machalek MA, Moorman NJ, Virgin HW. Interferons regulate the
phenotype of wild-type and mutant herpes simplex viruses in vivo. J Exp Med. 1999; 189(4):663–
672. [PubMed: 9989981]

Lupas A, Van Dyke M, Stock J. Predicting coiled coils from protein sequences. Science. 1991;
252(5010):1162–1164. [PubMed: 2031185]

Mahanty S, Bray M. Pathogenesis of filoviral haemorrhagic fevers. Lancet Infect Dis. 2004; 4(8):487–
498. [PubMed: 15288821]

Muhlberger E, Lotfering B, Klenk HD, Becker S. Three of the four nucleocapsid proteins of Marburg
virus, NP, VP35, and L, are sufficient to mediate replication and transcription of Marburg virus-
specific monocistronic minigenomes. J Virol. 1998; 72(11):8756–8764. [PubMed: 9765419]

Neumann G, Feldmann H, Watanabe S, Lukashevich I, Kawaoka Y. Reverse genetics demonstrates
that proteolytic processing of the Ebola virus glycoprotein is not essential for replication in cell
culture. J Virol. 2002; 76(1):406–410. [PubMed: 11739705]

Parisien JP, Lau JF, Horvath CM. STAT2 acts as a host range determinant for species-specific
paramyxovirus interferon antagonism and simian virus 5 replication. J Virol. 2002; 76(13):6435–
6441. [PubMed: 12050355]

Park MS, Garcia-Sastre A, Cros JF, Basler CF, Palese P. Newcastle disease virus V protein is a
determinant of host range restriction. J Virol. 2003; 77(17):9522–9532. [PubMed: 12915566]

Poole E, He B, Lamb RA, Randall RE, Goodbourn S. The V proteins of simian virus 5 and other
paramyxoviruses inhibit induction of interferon-beta. Virology. 2002; 303(1):33–46. [PubMed:
12482656]

Rahaman A, Srinivasan N, Shamala N, Shaila MS. Phosphoprotein of the rinderpest virus forms a
tetramer through a coiled coil region important for biological function. A structural insight. J Biol
Chem. 2004; 279(22):23606–23614. [PubMed: 15037604]

Sanchez, A.; Khan, AS.; Zaki, SR.; Nabel, GJ.; Ksiazek, TG.; Peters, CJ. Filoviridae: Marburg and
Ebola Viruses. In: Knipe, DM.; Howley, PM., et al., editors. Fields Virology. 4 ed. Vol. Vol. 1.
Philadelphia: Lippincott Williams and Wilkins; 2001. p. 1279-1304.

Schafer SL, Lin R, Moore PA, Hiscott J, Pitha PM. Regulation of type I interferon gene expression by
interferon regulatory factor-3. J Biol Chem. 1998; 273(5):2714–2720. [PubMed: 9446577]

Servant MJ, Grandvaux N, Hiscott J. Multiple signaling pathways leading to the activation of
interferon regulatory factor 3. Biochem Pharmacol. 2002; 64(5–6):985–992. [PubMed: 12213596]

Sharma S, tenOever BR, Grandvaux N, Zhou GP, Lin R, Hiscott J. Triggering the interferon antiviral
response through an IKK-related pathway. Science. 2003; 300(5622):1148–1151. [PubMed:
12702806]

Stevens J, Corper AL, Basler CF, Taubenberger JK, Palese P, Wilson IA. Structure of the uncleaved
human H1 hemagglutinin from the extinct 1918 influenza virus. Science. 2004; 303(5665):1866–
1870. [PubMed: 14764887]

Sullivan NJ, Peterson M, Yang ZY, Kong WP, Duckers H, Nabel E, Nabel GJ. Ebola virus
glycoprotein toxicity is mediated by a dynamin-dependent proteintrafficking pathway. J Virol.
2005; 79(1):547–553. [PubMed: 15596847]

Sumpter R Jr, Loo YM, Foy E, Li K, Yoneyama M, Fujita T, Lemon SM, Gale M Jr. Regulating Intracellular Antiviral Defense and Permissiveness to Hepatitis C Virus RNA Replication through a Cellular RNA Helicase, RIG-I. J Virol. 2005; 79(5):2689–2699. [PubMed: 15708988]

Tarbouriech N, Curran J, Ebel C, Ruigrok RW, Burmeister WP. On the domain structure and the polymerization state of the sendai virus P protein. Virology. 2000; 266(1):99–109. [PubMed: 10612664]

Towner JS, Paragas J, Dover JE, Gupta M, Goldsmith CS, Huggins JW, Nichol ST. Generation of eGFP expressing recombinant Zaire ebolavirus for analysis of early pathogenesis events and high-throughput antiviral drug screening. Virology. 2005; 332(1):20–27. [PubMed: 15661137]

Volchkov VE, Volchkova VA, Muhlberger E, Kolesnikova LV, Weik M, Dolnik O, Klenk HD. Recovery of infectious Ebola virus from complementary DNA: RNA editing of the GP gene and viral cytotoxicity. Science. 2001; 291(5510):1965–1969. [PubMed: 11239157]

Watanabe S, Watanabe T, Noda T, Takada A, Feldmann H, Jasenosky LD, Kawaoka Y. Production of novel ebola virus-like particles from cDNAs: an alternative to ebola virus generation by reverse genetics. J Virol. 2004; 78(2):999–1005. [PubMed: 14694131]

Wathelet MG, Lin CH, Parekh BS, Ronco LV, Howley PM, Maniatis T. Virus infection induces the assembly of coordinately activated transcription factors on the IFN-beta enhancer in vivo. Mol Cell. 1998; 1(4):507–518. [PubMed: 9660935]

Weaver BK, Kumar KP, Reich NC. Interferon regulatory factor 3 and CREBbinding protein/p300 are subunits of double-stranded RNA-activated transcription factor DRAF1. Mol Cell Biol. 1998; 18(3):1359–1368. [PubMed: 9488451]

Yang ZY, Duckers HJ, Sullivan NJ, Sanchez A, Nabel EG, Nabel GJ. Identification of the Ebola virus glycoprotein as the main viral determinant of vascular cell cytotoxicity and injury. Nat Med. 2000; 6(8):886–889. [PubMed: 10932225]

Yoneyama M, Kikuchi M, Natsukawa T, Shinobu N, Imaizumi T, Miyagishi M, Taira K, Akira S, Fujita T. The RNA helicase RIG-I has an essential function in double-stranded RNA-induced innate antiviral responses. Nat Immunol. 2004; 5(7):730–737. [PubMed: 15208624]

Young DF, Chatziandreou N, He B, Goodbourn S, Lamb RA, Randall RE. Single amino acid substitution in the V protein of simian virus 5 differentiates its ability to block interferon signaling in human and murine cells. J Virol. 2001; 75(7):3363–3370. [PubMed: 11238862]
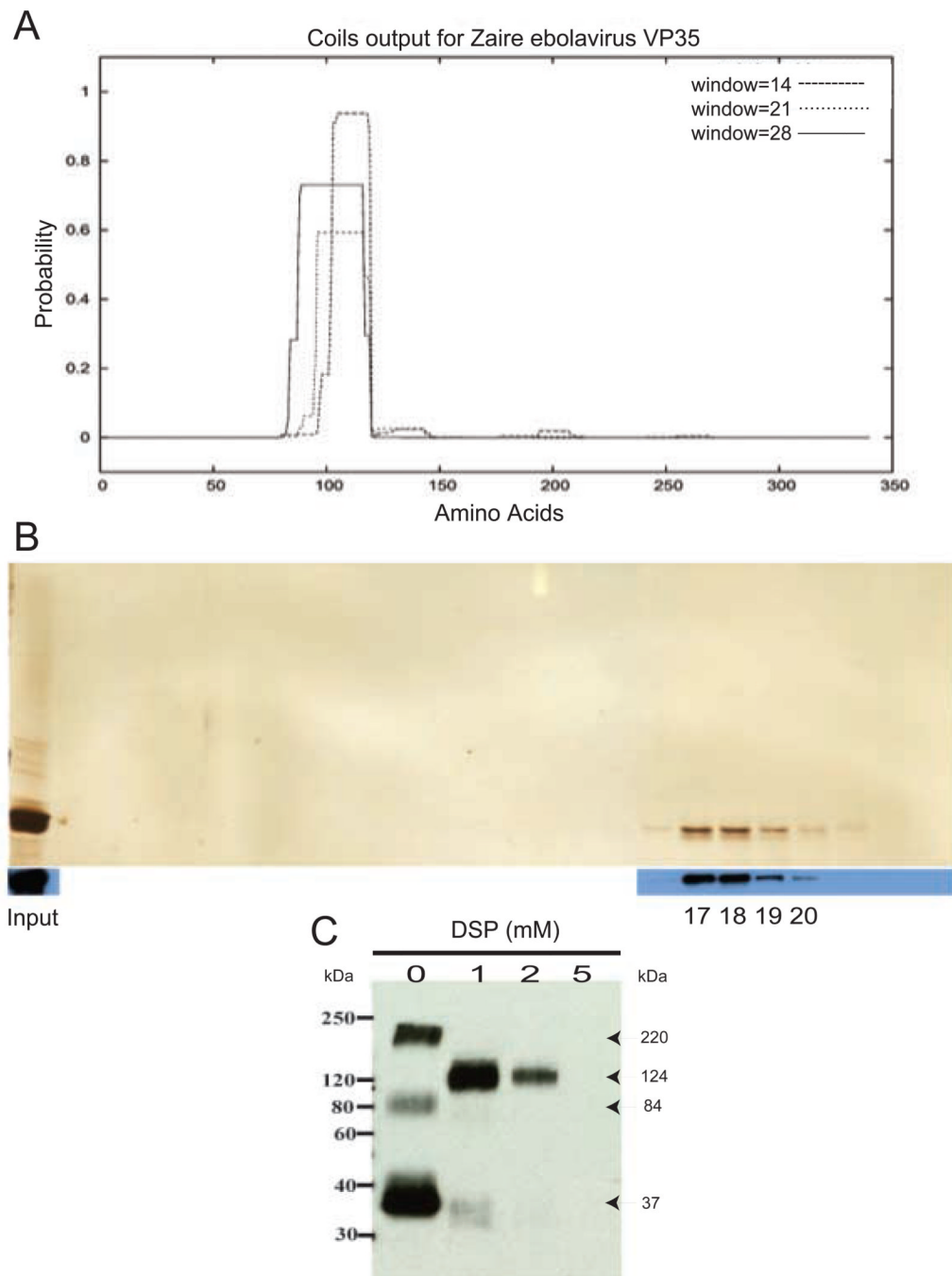
Figure 1. VP35 forms oligomers

(A) Output from analysis of the Zaire ebolavirus VP35 protein by the COILS program. The X-axis represents the 340 amino acid VP35 sequence, and the Y-axis represents the probability (with 1=100%) that an amino acid residue is within a coiled-coil region. Different size scanning windows are indicated by different lines as shown in the inset. Window sizes are 14 (dashed line), 21 (dotted line) and 28 (solid line) residues. (B) Gel filtration analysis of VP35. Purified FLAG-VP35 was fractionated on a Superdex-200 fast-performance liquid chromatography column (Amersham Biosciences). Collected gel filtration fractions were analyzed by silver stain (top) and by western blot with anti-VP35 monoclonal antibody (bottom). The indicated fractions correspond to the following

approximate molecular weights: fraction 17-194 kDa; 18-126 kDa; 19-81 kDa; and 20-52 kDa. Molecular weights were estimated by comparison to protein standards chymotrypsinogen A (19.9 kDa), bovine serum albumin (67 kDa), catalase (232 kDa), ferritin (440 kDa) and thyroglobulin (670 kDa), run under identical conditions. (C) DSP crosslinking analysis of VP35. Purified FLAG-VP35 was crosslinked with 0, 1, 2 or 5 mM DSP for 30 min and subsequently subjected to SDS-PAGE analysis under nonreducing conditions. The calculated molecular weights for each band are indicated by the arrows pointing to the corresponding band. Western blotting of gel filtration and crosslinking samples were performed using a monoclonal anti-VP35 antibody (6C5).
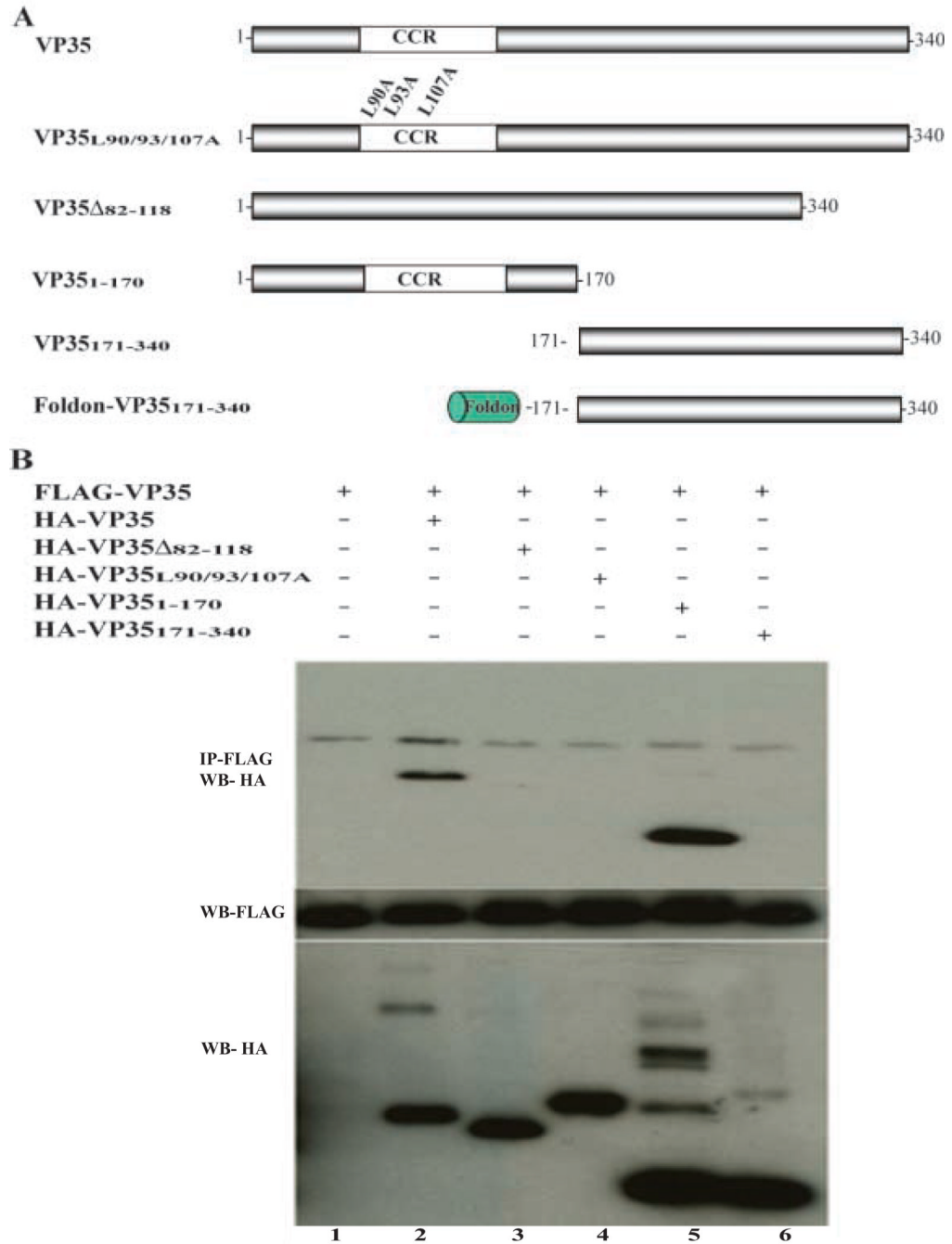
Figure 2. VP35-VP35 interaction requires the predicted coiled coil domain
(A) A schematic illustration of the wild-type and mutant forms of VP35 used for these experiments is presented. CCR, putative coiled-coil region. Foldon, foldon trimerization domain (see text). (B) 293T cells were transfected with expression plasmids encoding the indicated proteins. Twenty-four hours post-transfection cells were harvested and lysed. The prepared lysates were immunoprecipitated (IP) using anti-FLAG antibody (Sigma). After SDS-PAGE, western blotting was performed using anti-HA antibody (Sigma). Expression of HA and FLAG-tagged constructs were confirmed by Western blot analysis, with anti-HA and anti-FLAG tag antibodies, as is shown in the middle and lower panels. Note that

oligomeric forms of wt VP35 and VP35$_{1-170}$ molecules are seen in the lower panel depicting the anti-HA western blot of total cell lysates.
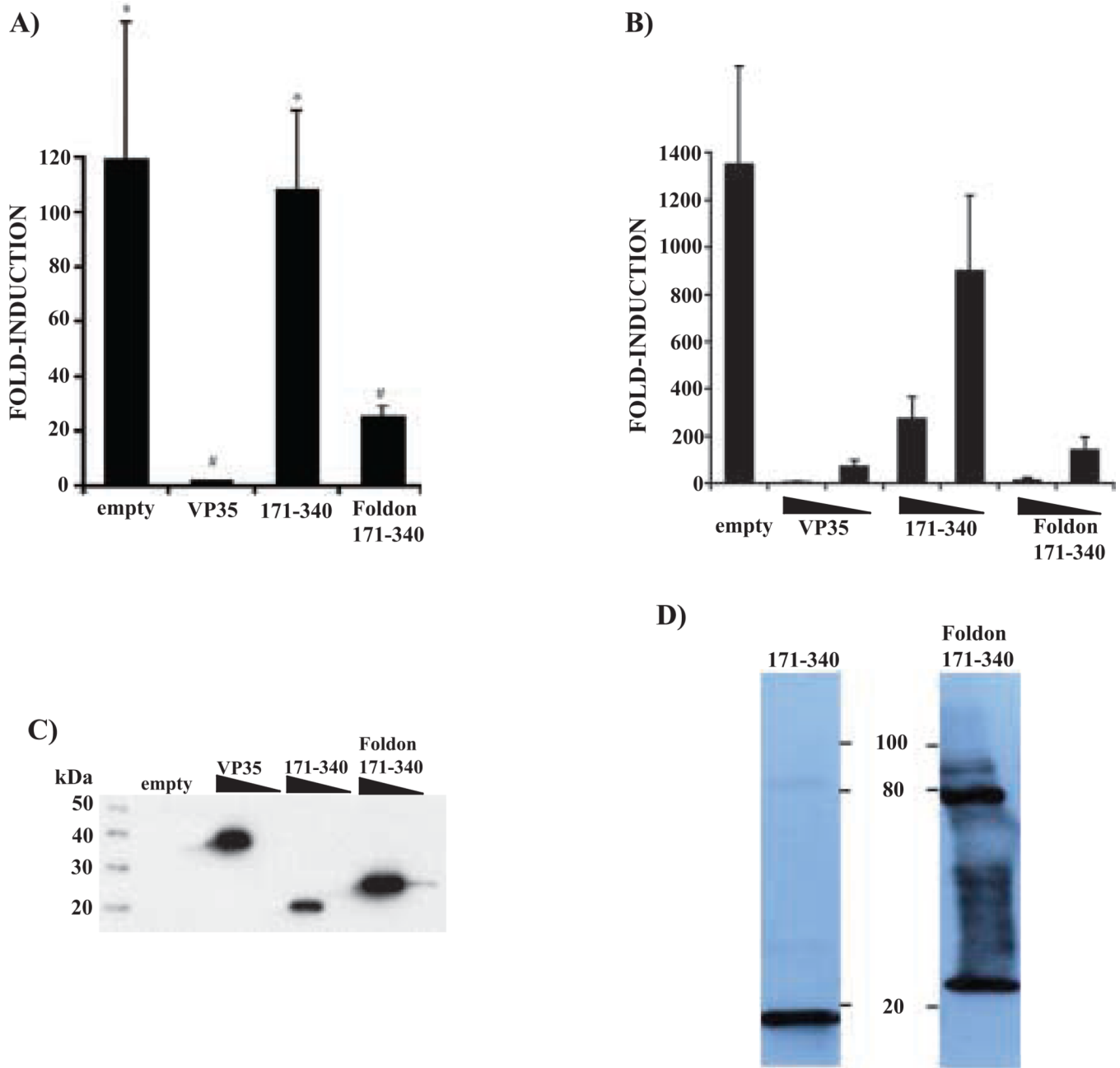
Figure 3. Ability of full length and mutant VP35 constructs to inhibit activation of IRF-3 responsive genes

(A, B) Cells were co-transfected with empty expression plasmid or plasmids expressing the indicated wild-type or mutant VP35s along with an ISG54 promoter-driven CAT reporter gene and a constitutively expressed *Renilla* luciferase reporter plasmid. One day post-transfection, the cells were infected with SeV (moi=10) and, the following day, reporter gene activity was measured. Virus-induced ISG54 reporter values were normalized to the luciferase activity of a *Renilla* luciferase expressing plasmid. Results are presented as fold-induction of the ISG54 reporter relative to an empty vector-transfected, mock-infected control. In panel A, all dishes received 2.5 μg of expression plasmid. In panel B, 25 or 250 ng of expression plasmid (expressing empty vector (empty), full-length VP35 (VP35),

VP35$_{171-340}$ (171–340) or Foldon-VP35$_{171-340}$) were transfected (concentrations indicated by wedges). For these experiments, empty vector was used to adjust all transfections to the same final DNA concentration. For both A and B, the error bars indicate standard deviation. In panel A, values not statistically different, as determined by a Student's t-test (P 0.05), are indicated by identical symbols (* and #). In panel B, the values for empty vector (empty)- and the 171–340 (lower 25 ng plasmid concentration)-transfected samples are statistically different from each other and all other samples, as determined by Student's t-test (P 0.05). (C) Western blot analysis of the indicated expression plasmids is provided (following transfection of 250 ng or 25 ng). The relative expression levels of these proteins are highly reproducible. (D) Expression of HA-VP35$_{171-340}$ and Foldon-HA-VP35$_{171-340}$ to verify trimer formation of Foldon-VP35$_{171-340}$ construct. Lysates from cells transfected with the indicated construct were subjected western blot analysis with anti- HA antibody (Sigma). These samples were not boiled prior to electrophoresis.
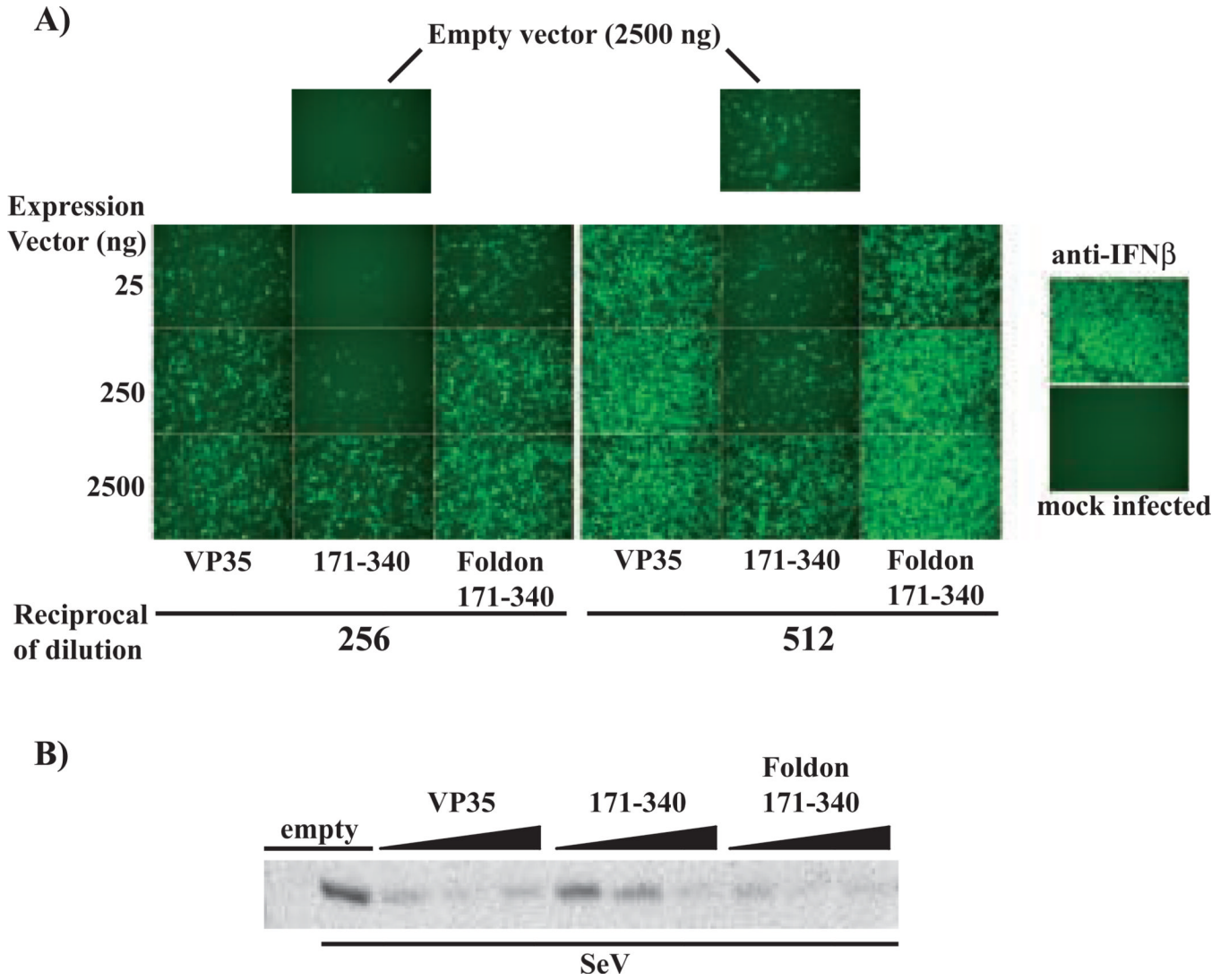
Figure 4. An interferon bioassay demonstrates that the foldon motif restores to VP35$_{171-340}$ the ability to inhibit endogenous IFNβ production

293T cells were transfected with the indicated amounts (left of the figure) of expression plasmids encoding VP35, VP35$_{171-340}$, and Foldon-VP35$_{171-340}$. The total amount of expression plasmid in all transfections was adjusted to a 2500 ng with empty vector. As a control, cells were transfected with 2500 ng empty vector (top two panels). 24 hours post-transfection, the 293T cells were mock infected or infected with SeV (moi=10). One day post-infection media supernatants from all cultures were collected, clarified by centrifugation and UV treated to inactivate any infectious SeV. A. To test for IFN antiviral activity, the inactivated supernatants were transferred onto Vero cells at the indicated dilutions (1:256 or 1:512, indicated by "Reciprocal of dilution"). The treated Vero cells were subsequently infected with the NDV-GFP virus. IFN present in the 293T cell supernatants, induced by the prior SeV infection, inhibits replication of NDV-GFP and green fluorescence in the Vero cells, (see the two uppermost panels, empty vector (2500 ng)). As the supernatnants are diluted, an increase in GFP expression is seen. In the anti-IFNβ panel, supernatant from an empty vector-transfected, SeV-infected cells was pre-incubated with IFNβ neutralizing antiserum prior to its addition to the Vero cells. The recovery of NDV-GFP replication in these cells demonstrates that the antiviral effect in these cells is mediated

mainly by IFNβ. The "Mock infected" control panel denotes Vero cells without NDV-GFP infection. VP35, 171–340 and Foldon 171–340 indicate the expression plasmids transfected at the indicated amount (in ng/10^6 cells) (see Expression vector amounts at left). B. To assess SeV-induced expression of the IRF-3-responsive ISG56 gene, western blots were performed to examine levels of p56, the protein product of the ISG56 gene. Expression of p56, 1 day post SeV-infection of cells tranfected with 25, 250 or 2500 ng of the indicated expression plasmids, is shown.
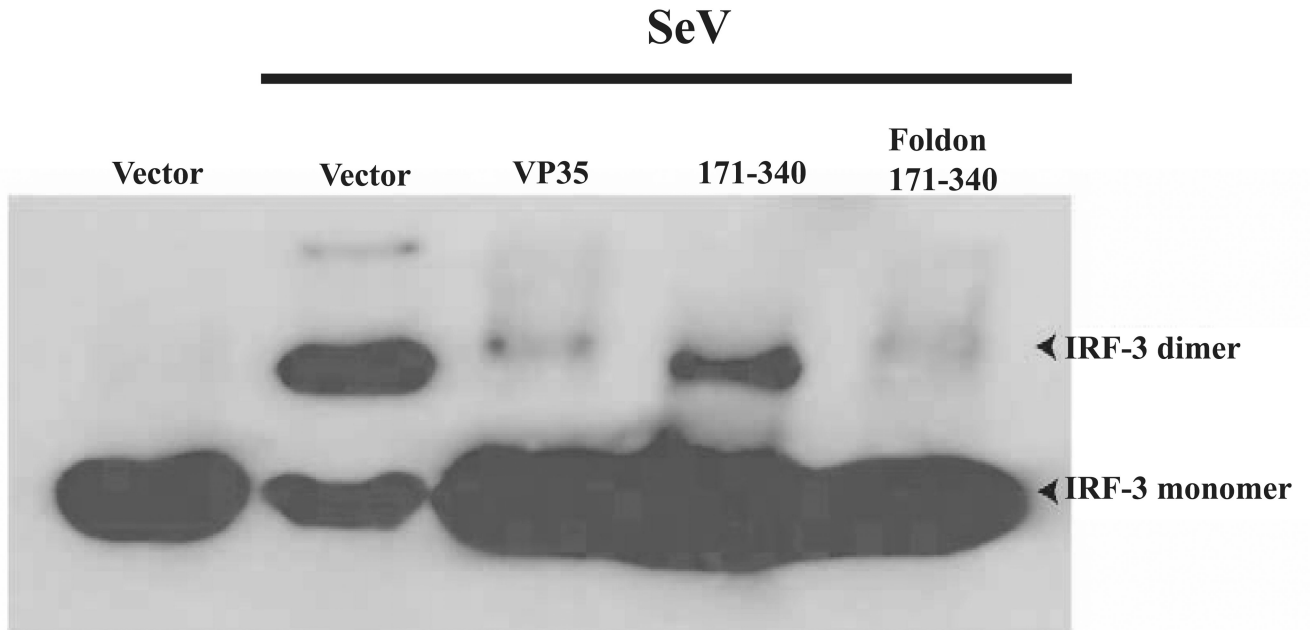
Figure 5. The foldon trimerization motif restores the ability of VP35$_{171-340}$ to block IRF-3 activation
293T cells were transfected with the indicated protein expression plasmids (full length VP35 (VP35), VP35$_{171-340}$ (171–340) or Foldon-VP35$_{171-340}$ (Foldon 171–340) and either mock-infected of infected with Sendai virus (SeV) 24hr post-transfection. Ten hours post-infection cells were harvested and lysed. For IRF-3 analysis, cells were subjected to native PAGE analysis as previously described (Iwamura reference) followed by blotting with an anti-IRF-3 monoclonal antibody.